Proton/Hydrogen Transfer Affects the S-State-Dependent Microsecond Phases of $P680^+$ Reduction during Water Splitting†

Maria J. Schilstra,‡ Fabrice Rappaport,§ Jonathan H. A. Nugent,|| Christopher J. Barnett,‡ and David R. Klug*,‡

Molecular Dynamics and Photosynthesis Research Groups, Centre for Photomolecular Sciences, Department of Biochemistry and Chemistry, Imperial College, London SW7 2AY, United Kingdom, Institut de Biologie Physico-Chimique, 13 rue Pierre et Marie Curie, 75005 Paris, France, and Department of Biology, Darwin Building, University College, Gower Street, London WC1E 6BT, United Kingdom

Received June 10, 1997; Revised Manuscript Received December 18, 1997

ABSTRACT: To investigate a possible coupling between $P680^+$ reduction and hydrogen transfer, we studied the effects of H_2O/D_2O exchange on the $P680^+$ reduction kinetics in the nano- and microsecond domains. We concentrated on studying the period-4 oscillatory (i.e., S-state-related) part of the reduction kinetics, by analyzing the *differences* between the $P680^+$ reduction curves, rather than the full kinetics. Earlier observations that $P680^+$ reduction kinetics have microsecond components were confirmed: the longest observable lifetime whose amplitude showed period-4 oscillations was 30 μs. We found that solvent isotope exchange left the nanosecond phases of the $P680^+$ reduction unaltered. However, a significant effect on the oscillatory microsecond components was observed. We propose that, at least in the S_0/S_1 and S_3/S_0 transitions, hydrogen (proton) transfer provides an additional decrease in the free energy of the $Y_Z{}^+P680$ state with respect to the Y_ZP680^+ state. This implies that relaxation of the state $Y_Z{}^+P680$ is required for complete reduction of $P680^+$ and for efficient water splitting. The kinetics of the $P680^+$ reduction suggest that it is intraprotein proton/hydrogen rearrangement/transfer, rather than proton release to the bulk, which is occurring on the 1−30 μs time scale.

The process of water splitting by photosystem II (PS-II)[1] involves the excitation of the primary electron donor P680, and rapid electron transfer from the singlet excited-state P680* to the bound plastoquinone, Q_A, to form the relatively stable $P680^+Q_A{}^-$ state ($\Delta G \approx -450$ meV). The cation $P680^+$ extracts an electron from water bound to the manganese cluster that forms the oxygen-evolving complex (OEC), via the electron donor Y_Z, tyrosine-161 on the reaction center polypeptide D1. Sequential excitations of P680 and withdrawal of electrons cause the OEC to cycle between the five S-states, S_0 to S_4. During the S-state cycle, two molecules of water bind to the OEC. S_4 converts spontaneously to S_0, releasing one molecule of O_2. In the dark, the S_2- and S_3-states decay to S_1 within a few minutes. On further dark adaptation, the S_0- and S_1-states equilibrate, S_0 being slowly oxidized by a second redox-active tyrosine, Y_D, tyrosine-160 on the D2 reaction center polypeptide. During the S-state cycle, four protons are released to the lumenal side of the thylakoid membrane. In vivo, this release of protons into the lumen, together with proton uptake at the stromal site, creates a pH gradient across the membrane. In thylakoids and granal stack membranes, the proton release is noninteger, and dependent on the pH. Proton release stoichiometries and kinetics are reviewed in (*1*, *2*), and see also (*3*−*5*). For reviews of O_2 evolution by PS-II, see (*6*−*10*).

It is well established that the majority of $P680^+$ is reduced by Y_Z within 1 μs in particles which are fully active in water splitting [(*7*) and references cited therein]. The reduction rate in the nanosecond time domain is dependent on the S-states. Values for the main kinetic component of the $P680^+$ decay for the S-state transitions S_0/S_1 and S_1/S_2 have been reported as 20−60 ns at pH 6.5 (*11*−*15*). Components of approximately 50 and 300 ns were distinguished for the S_2/S_3 and S_3/S_0 transitions (*11*, *12*). Furthermore, several investigators have communicated the observation of longer lived $P680^+$ in water-splitting complexes. Kinetic components with lifetimes varying from 1.4 to 35 μs have been reported (*13*, *15*, *16*). However, the existence and interpretation of microsecond components in the reduction of $P680^+$ has been the subject of much debate [(*11*−*13*, *16*−*22*); see Discussion]. The rate of electron transfer from the OEC to $Y_Z{}^+$ is much slower, and also strongly S-state-dependent. Lifetimes of <3−250 μs have been reported for the transition $Y_Z{}^+S_0/Y_ZS_1$, 30−140 μs for $Y_Z{}^+S_1/Y_ZS_2$, 100−600 μs for $Y_Z{}^+S_2/Y_ZS_3$, and 1−4.5 ms for $Y_Z{}^+S_3/Y_ZS_0$ [(*23*) and references cited therein].

Convincing evidence has been presented that the fastest proton release into the bulk can take place only in tens of microseconds after the excitation (*2*, *3*). This means that,

† This work was supported by the Biotechnology and Biological Sciences Research Council, and the European Community (Human Capital and Mobility program).

* To whom correspondence should be addressed. Telephone: 44 171 594 5806. Fax: 44 171 594 5806.

‡ Imperial College.

§ Institut de Biologie Physico-Chimique.

|| University College.

[1] Abbreviations: PS-I, photosystem I; PS-II, photosystem II; BBY, granal stack membrane particles containing PS-II; DCBQ, 2,6-dichlorobenzoquinone; DCMU, 3-(3,4-dichlorophenyl)-1,1-dimethylurea; fwhm, full width at half-maximum; IC, Imperial College London; MES, 2-(*N*-morpholino)ethanesulfonic acid; P_{700}, chlorophyll *a* primary electron donor in PS-I; P680, chlorophyll *a* primary electron donor in PSII; SMNCB, buffer containing 20 mM MES, pH 6.5, 10 mM NaCl, 5 mM $CaCl_2$, 0.3 M sucrose; UCL, University College London.

S0006-2960(97)01381-0 CCC: $15.00
Published on Web 02/24/1998

in some of the transitions, proton release *precedes* the actual S-state transition. In that case, one might expect proton release to be coupled to $P680^+$ reduction and Y_Z oxidation.

In this paper, we present a study of the coupling between electron and proton or hydrogen transfer during the reduction of $P680^+$. Because of the ambiguity in the literature about the occurrence of long-lived $P680^+$ in water splitting, we decided to carry out a reinvestigation of the $P680^+$ reduction kinetics in the microsecond time range. We were able to achieve sufficient accuracy to determine the kinetics in this time domain (10−200 μs) in greater detail than obtained before. Much of the ambiguity has arisen because particular recombination events in particles that do not evolve oxygen occur on the same time scale as processes related to water splitting. To avoid misinterpretation of the data, our analysis has concentrated solely on the period-4 oscillatory parts of the kinetics. This part of the kinetics is necessarily S-state-dependent, and is thus only associated with fully functional water splitting. Our results confirm that the oscillatory behavior does indeed extend far into the microsecond domain.

Furthermore, we investigated the effect of H_2O/D_2O exchange on the kinetics of $P680^+$ reduction over a time range of up to 45 μs after the excitation. Two groups have reported that H_2O/D_2O exchange has no effects on Y_Z to $P680^+$ electron-transfer rates in the water splitting process (*14*, *24*), but their investigations of the S-state-related kinetics extended only up to 1 μs. We find that there is indeed little isotope effect on processes that occur in the nanosecond time domain. However, we observed that the solvent isotope exchange results in a significant change in the oscillatory components of $P680^+$ reduction in the microsecond time domain.

MATERIALS AND METHODS

Materials. Oxygen-evolving PS-II-enriched granal membranes (also termed BBYs) were prepared both at Imperial College (IC) and at University College (UCL) for comparison. Samples were prepared from marked spinach (IC, UCL) or freshly cropped 10−14 day old pea seedlings (UCL) according to the method of (*25*), using Triton X-100, with the modifications of (*3*) (IC) or (*26*) (UCL). Control rates of oxygen evolution at 25 °C, measured both in H_2O and in D_2O buffers in a Clark-type oxygen electrode, were 400−800 μmol of O_2 (mg of chlorophyll)$^{-1}$ h^{-1}, using DCBQ (IC), ferricyanide, or dimethylbenzoquinone (UCL) as electron acceptors. The membranes were stored at −80 °C at a chlorophyll concentration of 4 mg/mL in a buffer containing 20 mM MES, pH 6.5, 5 mM $MgCl_2$, 10 mM NaCl, 5 mM $CaCl_2$, and 0.3 M sucrose (SMNCB, IC) or in liquid N_2 in 20 mM MES, pH 6.5, 15 mM NaCl, 5 mM $MgCl_2$, 0.4 M sucrose (UCL). The preparations were checked for contamination with photosystem I (PS-I) by EPR detection of $P700^+$ (UCL) or by comparing the average $P680^+$ decays (see below) in the absence and presence of tungsten octocyanate (WCN, at IC). WCN has a midpoint potential of +570 mV, and effectively eliminates the contribution of the $P700^+$ decay to the observed curves. No detectable contamination with PS-I was found in the preparations used in this study. The effect of DCMU on the membranes prepared at IC was tested as described in (*27*). No significant fraction of DCMU-insensitive particles was detected in the absence of any secondary acceptors. DCBQ (2,6-dichlorobenzoquinone) was purchased from Kodak, and D_2O (99.9% atom D) from Sigma Chemical. WCN was a kind gift of Dr. A. Stemler (Institut de Biologie Physico-Chimique, Paris, France). All other reagents used were analytical grade. Stock solutions of DCBQ (50 mM) were prepared in ethanol (96%) and stored at −20 °C in the dark for no longer than 1 month. The SMNCB used to dilute the stock PS-II preparation was made up in H_2O or D_2O. The pD in the D_2O buffer was adjusted to 6.1 (pH meter reading), to correct for differences in sensitivity to H^+ and D^+ ions of the pH meter (*28*). A 1% (w/v) stock solution of Triton X-100 was also prepared using either H_2O or D_2O.

Equipment. Samples were excited by saturating flashes from a Q-switched frequency-doubled Nd:YAG laser (λ = 532 nm, 20 mJ·cm^{-2}, flash frequency 2 Hz unless stated otherwise). $P680^+$ decays were monitored by the absorption at 830 nm of a probe beam perpendicular to the exciting beam with either a microsecond or a nanosecond resolution measurement system. Measurements on the 10−500 μs time scale were taken on a versatile system with a tungsten halogen source, monochromators before and after the sample, and a continuously biased photodiode DC-coupled into a preamplifier with offset. For the faster time scales, a 35 mW 830 nm continuous-wave diode laser was employed as a source, and the probe beam was detected via a filter by a photodiode (EG&G FND100) with gated bias and a DC-restored video amplifier. Exclusion of scattered excitation light and fluorescence were accomplished by the appropriate combinations of transmission and spatial filters. The instrument response functions (full width at half-maximum, fwhm) were 10 ns in the diode laser setup, and 1 μs in the tungsten lamp configuration. The signal was transferred from the detector to a 400 Ms/s, 100 MHz oscilloscope (Gould 4072), and from there, via an IEEE 488 instrumentation interface, to a PC. Each decay in a train of N_{flash} excitations was stored individually (1008 channels per data set). The standard deviation of the pretrigger signal was taken as the background noise level. Its value varied owing to day-to-day differences in the performance of the equipment, but was typically around 4×10^{-5} (diode laser setup) or 8×10^{-5} (tungsten lamp setup) *A* unit after a single flash. Typically, 20 (diode laser) or 80 (tungsten lamp) sets of N_{flash} curves, each set obtained with a fresh, dark-adapted sample, were averaged per flash, decreasing the noise level to approximately 1×10^{-5} absorption unit. Initial absorption values (measured at 10 ns after the flash) were 1.0×10^{-3} to 1.4×10^{-3} absorption unit. The differences between the curves were maximal in the first 5 flashes at about 50 ns after the flash, and were about 2×10^{-4} to 3×10^{-4} absorption unit.

Sample Preparation and Measurements. The BBY preparation was diluted with SMNCB to a final chlorophyll concentration of 80 μg/mL, and placed in a 4 mm × 4 mm fluorescence cuvette. To reduce the light scattering caused by large aggregates of membrane fragments, and thus to increase the signal-to-noise ratio, a minimal amount of Triton X-100 (in H_2O or D_2O as appropriate) was added. The amount of Triton required to increase the transmission at 830 nm from 20% to about 80% was found to be approximately 0.2% (w/v) of Triton/mg of chlorophyll (i.e., 0.016% at [chlorophyll] = 80 μg/mL), and this was the Triton concentration used in all experiments. Data obtained

in the presence of up to 0.3% Triton/mg of chlorophyll were not significantly different from data obtained in the absence of any additional Triton, but higher concentrations of Triton did change the kinetics. Immediately prior to the measurement, DCBQ was added to a final concentration of 50 μM. The concentration of ethanol in the sample was always 0.2% (v/v) or less. It was found that concentrations of up to 0.5% ethanol had no effect on the course of the reaction.

Transient absorption spectra of the sample at 20 and at 200 μs after the flash had a peak around 830 nm, and were characteristic for $P680^+$. These spectra showed little or no contribution from $^3P680$ (*29*). To establish the excitation beam power required for saturation of the sample, $P680^+$ decay curves were collected at beam intensities varying from 2 to 25 mJ/pulse. The optimal beam power (>90% saturation, but as little fluorescence as possible) was found to be 10 mJ/pulse.

Preliminary experiments indicated that application of a saturating preflash, followed by a short period of dark adaptation to synchronize the PS-II membranes in S1, had no significant effect. Therefore, and in order to avoid introducing errors due to variations in dark-adaptation times, we did not preflash the membranes. It was found that varying the flash frequency between 0.5 and 3 Hz had no significant effect on the results. The magnitude of the miss factor (see below) varied, from preparation to preparation, between about 0.05 and 0.2. To be able to compare the measurements carried out in H_2O and D_2O, the experimental conditions had to be as similar as possible. To achieve this, we prepared H_2O and D_2O samples from the same concentrated BBY preparation, and performed the measurements on the same day. In this way, possible differences due to variations in instrumental characteristics and biological material were minimized. The H_2O concentration in the D_2O samples was 2%. We considered the possibility that some of the H^+/D^+ exchange in BBYs in D_2O may take place only during turnover. In order to investigate this possibility, we gave some D_2O samples 20 saturating preflashes, and subsequently allowed them to dark-adapt for 30 min. We did not detect any significant differences between the data collected with the untreated and with the preilluminated samples.

Data Analysis. In the text below, the following symbols will be used: N_{flash}, total number of flashes in an excitation sequence; $A(t,n)$, absorption at 830 nm, at time t, after the nth flash in a sequence of excitations; $A_{avg}(t)$, absorption at 830 nm, averaged over all flashes except flash 1; $\Delta A(t,n)$, deviation from average $A(t,n)$ [$\Delta A(t,n) = A(t,n) - A_{avg}(t)$]. Note that $A(t,n)$ and $A_{avg}(t)$ have equal, nonoscillatory contributions of $P680^+$ in particles that are inactive in water splitting, and therefore the difference curves, $\Delta A(t,n)$, have no such contribution.

(*A*) *Autocorrelation Analysis*. The autocorrelation C at lag j of a sampled function f_k, periodic with period N, is defined as

$$C_j \equiv \sum_{k=0}^{N-1} (f_{j+k} \times f_k)$$

(*30*).

Autocorrelation analysis suppresses nonperiodic noise, and emphasizes the periodic character of the data while removing confusions caused by damping of the oscillations. In the context of these studies, taking the autocorrelation of the data has the effect of averaging over a sequence of multiple flashes to obtain the period-4 behavior more clearly and with higher effective signal-to-noise. Autocorrelation functions were calculated from the full $A(t,n)$ data sets, over $n = 2$ to N_{flash}, for each point t in time. To remove the nonoscillatory information, the interpretation of which is ambiguous, the average kinetics are subtracted. The autocorrelation data with the average kinetics subtracted are denoted as $\Delta C(t,n)$.

(*B*) *Global Analysis*. Curves were analyzed as multiexponential decays, using a global analysis program developed in our laboratory by T. Rech and M. Bell. The program uses the Marquardt algorithm for nonlinear least-squares fitting (*31*). It enabled us to determine a single set of best-fit parameters for data collected on different time scales, and also to link together lifetimes or amplitudes throughout the sets of $\Delta A(t,n)$ and $\Delta C(t,n)$, to produce a global analysis of all of the data.

(*C*) *Data Decomposition.* S-State decomposition of the data was carried out as described in reference (*32*), using a general linear least-squares routine [subroutine LFIT (*30*)]. In the calculations, we used a value of 0.1 for the fraction of particles in the S_0-state after dark-adaptation, on the basis of an average value determined by Rappaport et al. (*3*) for PS-II-enriched granal membranes prepared from spinach. We found, however, that variations of ± 0.1 in this value did not result in significantly different solutions. Under the conditions of our measurements (YAG laser flash ~6 ns fwhm), the chance that a double hit occurs is negligible, and we have, therefore, assumed that the double-hit parameter, β, is zero. Values of α, the miss parameter, were estimated from the sets of N_{flash} data using two methods. The first method uses the equations derived by Lavorel (*33*). However, we noticed that the value of α estimated from Gaussian noise alone using this method was 0.11 ± 0.06. We observed a tendency toward 0.11 for the values of α estimated at each point in time from the $(\Delta)A(t,n)$ data sets, dependent on the signal/noise ratio. Therefore, values of α were also estimated by S-state decomposition of the data for a range of values of α, and determining which value of α gave the lowest chi-square. This method gave unbiased values for α in calculations of simulated noisy data.

RESULTS

General. Rather than analyzing the full $P680^+$ reduction kinetics, we have concentrated on studying the *differences* between individual curves within the sets. This was done by subtracting the average $P680^+$ reduction curves, $A_{avg}(t)$, from the individual curves $A(t,n)$ at each point t in time, and globally analyzing the resulting $\Delta A(t,n)$ curves. Particles that are inactive in water splitting (further indicated as "inactive particles") do not show period-4 oscillations, and their contribution to the kinetics is the same in each curve. By subtracting the average $P680^+$ reduction kinetics from the individual curves, the contributions of inactive particles disappear. Period-4 oscillations were clearly visible in each set of $\Delta A(t,n)$. The periodic character of each data set was further studied by autocorrelation analysis. Autocorrelation analysis is a useful method for extracting periodicity in the data, and suppressing nonperiodic noise.

The deviations from the average $P680^+$ reduction kinetics, as shown in Figures 1a, 2c, and 2d, indicate that (1) the different S-states deviate from the average kinetics in a variety of ways at different times; (2) the amplitude of the S-state oscillations damp over time (as well as with flash number) with no oscillatory component detectable beyond about 100 μs. Global analysis of the $\Delta A(t,n)$ and the autocorrelation data $\Delta C(t,n)$ allows us to determine the time constants with which the S-state oscillations are damped. We emphasize that our analysis is restricted to the oscillatory components of the data only. The average kinetics are subtracted, and we make no analysis or interpretation of the average $P680^+$ kinetics in this paper.

Long-Lived Oscillatory Components in the $P680^+$ Reduction Kinetics. To study a possible connection between the electron- and proton-transfer processes, it was necessary to investigate $P680^+$ reduction kinetics in the microsecond domain in greater detail than before. Figure 1a shows the deviations from average of the $P680^+$ reduction kinetics, obtained after flashes $n = 2-5$, on a time scale up to 200 μs. The average concentration of $P680^+$ at 50 μs ($A_{830} \approx 0.11 \times 10^{-3}$) was about one-tenth of the initial $P680^+$ concentration ($A_{830} = 1.1 \times 10^{-3}$). The data were further subjected to an autocorrelation analysis. The deviations from average, $\Delta A(t,n)$, and the autocorrelation curves, $\Delta C(t,n)$, were globally analyzed as single-exponential functions. The lifetime of the oscillatory component was 30 μs, and its amplitudes are shown in Figure 1b,c. The miss factor, estimated from these data, was 0.06 ± 0.01. As expected, the autocorrelation analysis has emphasized the period-4 character of the oscillations.

Effect of D_2O. We compared the $P680^+$ reduction kinetics in H_2O and D_2O, both in the nanosecond and in the microsecond time ranges, to further investigate a possible coupling between electron transfer from Y_Z to $P680^+$ and proton transfer (because of instrumental limitations, we monitored the $P680^+$ reduction kinetics up to 45 μs only in this experiment). To be able to compare details of the $P680^+$ reduction in the two solvents, measurements in H_2O and in D_2O were performed under experimental conditions that were as similar as possible (see Materials and Methods).

Figure 2a,b shows the full $P680^+$ reduction kinetics after flashes 2−5 in H_2O and D_2O. $P680^+$ reduction in D_2O is slower than in H_2O. It is possible, however, that this effect is partly, or wholly, due to the presence of inactive particles. Haumann et al. (*24*) have studied the effect of D_2O on particles that had been exposed to high pH, and, as a result, had lost their oxygen-evolving activity. The authors report that the lifetimes of two microsecond components in the $P680^+$ reduction kinetics of the inactived particles slowed from 6 and 35 μs in H_2O to 15 and 60 μs in D_2O. However, by analyzing only the oscillatory parts of our data, we are able to circumvent any changes in kinetics caused by the isotope effect on inactive centers. The deviations from the average kinetics from 0.01 to 45 μs, after flashes 2−5, are shown in Figure 2c,d. The major difference between the data in H_2O and D_2O seems to develop from about 1 μs onward.

The deviations from average, $\Delta A(t,n)$, and the results of the autocorrelation analysis, $\Delta C(t,n)$, were globally analyzed. Four exponentials and an offset (i.e., a component whose lifetime was too long to be determined with any accuracy) were required to describe the data. Analysis of the data with three exponentials and an offset gave a nonrandom distribution of residuals, whereas analysis with more than five exponentials did not improve the fit. The lifetimes of the oscillatory components 1−4, both in H_2O and in D_2O, were 20 ns, and 0.11, 0.6, and 8 μs. To simplify the analysis and interpretation of these data, we discuss only the aggregate amplitudes $A_{23} = A_2 + A_3$ and $A_{45} = A_4 + A_5$. Further

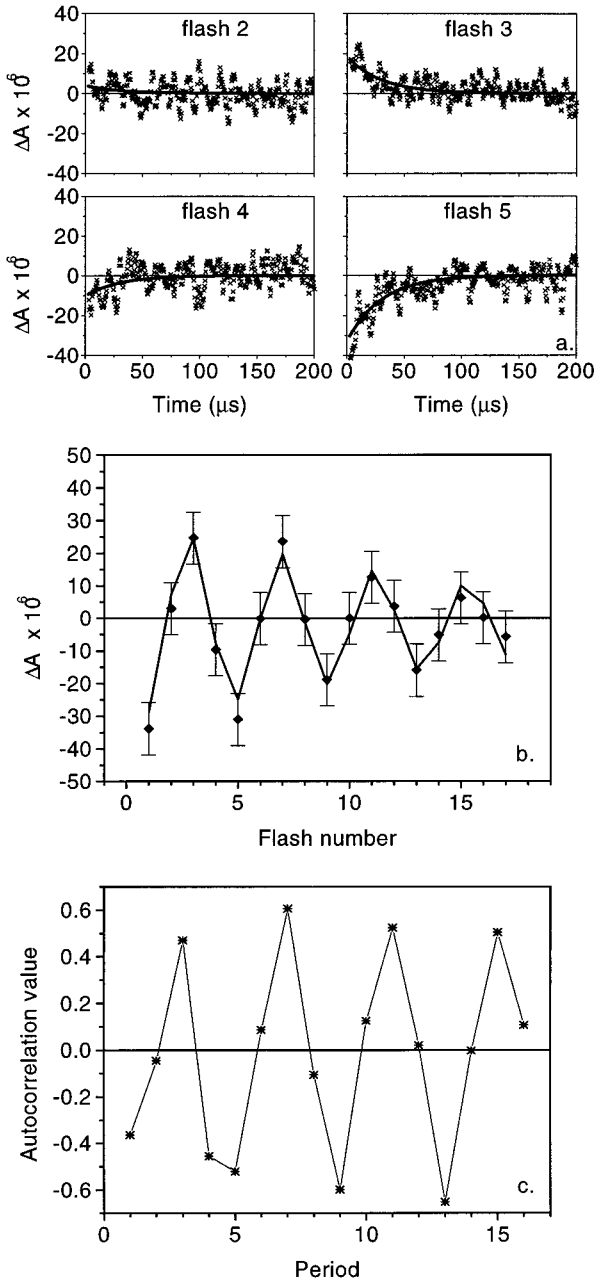

FIGURE 1: $P680^+$ reduction kinetics in the microsecond time domain. Data were collected on a single time scale (10−450 μs; 0.5 μs/channel); curves are averages of 80 excitations. (a) Deviations from the average $P680^+$ reduction kinetics after flashes 2−5 (average kinetics calculated over flashes 2−17). Solid lines indicate the results of a least-squares fit to single-exponential functions, all with 30 μs lifetimes. (b) (◆) amplitudes of the 30 μs component as a function of flash number. Error bars indicate the standard deviation of the data in the original curves (8×10^{-6}). (c) Amplitudes of the 30 μs component in the autocorrelation kinetics. Solid lines in (b) connect the calculated amplitudes, obtained from an S-state decomposition of the observed amplitudes, using a miss factor of 0.06; lines in (c) are merely drawn to guide the eye.

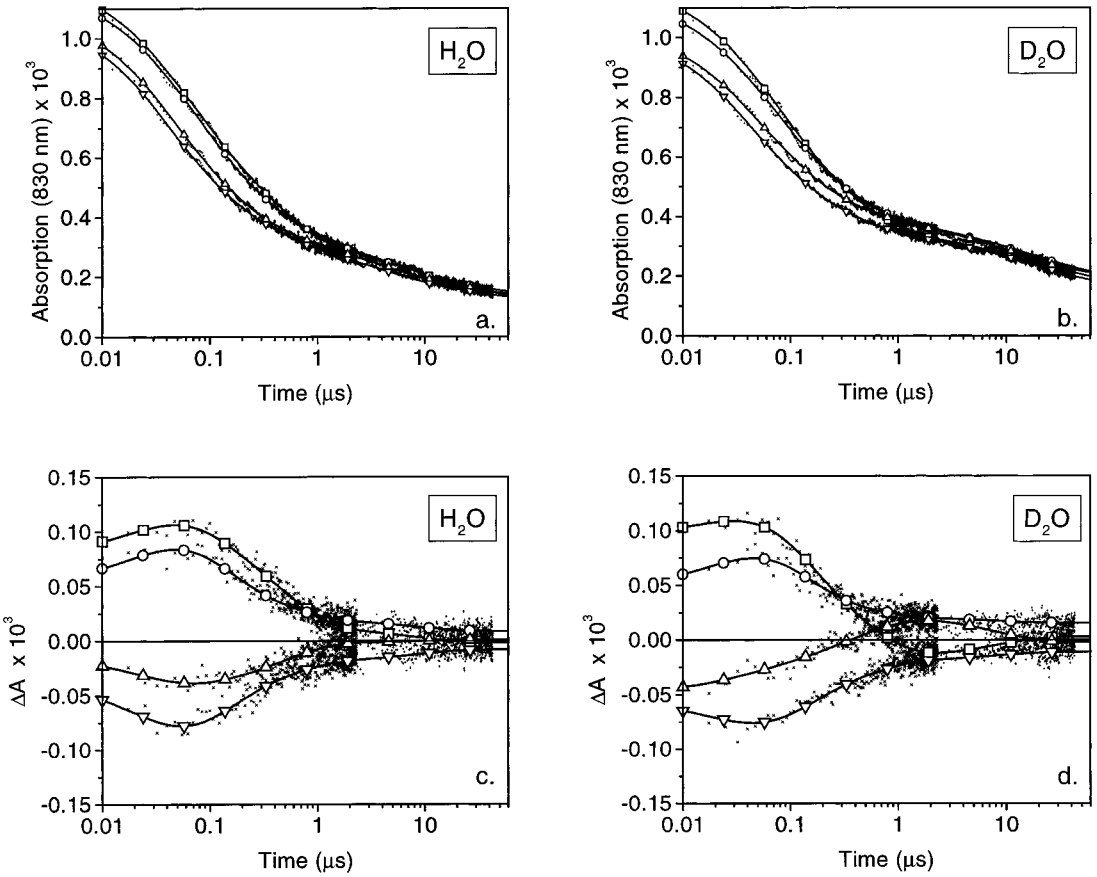

FIGURE 2: $P680^+$ reduction kinetics in H_2O and D_2O from 15 ns to 45 μs. Data are averages of 20 excitations, and were collected on 2 time scales (0.015−2.0 μs, 2.5 ns/channel; 0.1−45 μs, 50 ns/channel). (a, b) Full kinetics. (c, d) Deviations from average kinetics (average kinetics calculated over flashes 2−21). (a, c) Data in H_2O. (b, d) Data in D_2O. Solid lines represent the best fit of the data to multiexponential functions. Symbols have been plotted to distinguish the curves: squares, flash 2; circles, flash 3; up triangles, flash 4; down triangles, flash 5. The solid lines in (a) and (b) are the result of an overparametrized fit, and are indicated only to guide the eye. The solid lines in (c) and (d) are the results of the global analysis described in the text.

analysis and interpretation is somewhat involved, and beyond the scope of this paper. These details will be addressed in future work.

The values of A_1, A_{23}, and A_{45} in H_2O and D_2O are compared in Figure 3. The autocorrelation analysis has again emphasized the period-4 character of the kinetic components. Figure 2a−d shows that the oscillations of the nanosecond component amplitudes A_1 and A_{23} were, within experimental error, equal in the two isotopes of water. However, it is clear from Figure 2c,d that the microsecond amplitudes A_{45} are significantly different in H_2O and D_2O. The differences are most pronounced after flashes 2, 4, and 6. Furthermore, the maxima and minima have shifted from flash n in H_2O to flash $n+1$ in D_2O.

The miss factor, both in H_2O and in D_2O, was 0.18 ± 0.02. As mentioned above, the amplitudes plotted in Figures 1c ('A_{30}'), 2a (A_1), 2c (A_{23}), and 2e (A_{45}) were decomposed into the amplitudes of the individual S-state transitions, and then reconstituted to give the amplitudes connected by the lines. The S-state-decomposed values of A_{30} (miss factor 0.06) were very similar to those of A_{45} in H_2O (miss factor 0.18). In Figure 4, the S-state-decomposed values of A_{45} in H_2O and D_2O are compared.

DISCUSSION

We have investigated the reduction kinetics of $P680^+$ in dark-adapted PS-II-enriched granal stack membranes (BBY) in H_2O and D_2O. In our analysis, we concentrated on the period-4 oscillatory, S-state-dependent part of the curves. The following observations were made. (1) In water-splitting centers, a considerable concentration of $P680^+$ still is present at tens of microseconds after light absorption. (2) There is a significant isotope effect on the oscillatory microsecond phases of the reduction. This means that the microsecond phases are associated with proton/hydrogen motion as well as $P680^+$ reduction.

Comparison with Previous Observations. Period-4 oscillating components with lifetimes below 1 μs have been observed before by many investigators (see the introduction). Our data are largely in agreement with these previous observations. Oscillating components with lifetimes greater than 1 μs have also been observed in several previous studies [(*13*, *15*), and, in particular, (*16*)]. Unfortunately, the conclusions in two of those studies (*15*, *16*) were based upon the information in 5 flashes only, whereas the data presented in the other paper (*13*) included 8 flashes, but did not extend beyond 1 μs. The S-state dependence of a 35 μs component initially reported by Witt's group (*16*) was later questioned (*17*, *18*). However, the patterns of differences in the amplitudes of the observed >1.4 μs (*13*) and 35 μs (*16*) components are similar to the pattern that we found. The pattern found by Lukins et al. (*15*) is quite different from the patterns reported in the two studies mentioned above (*13*, *16*), and in this paper.

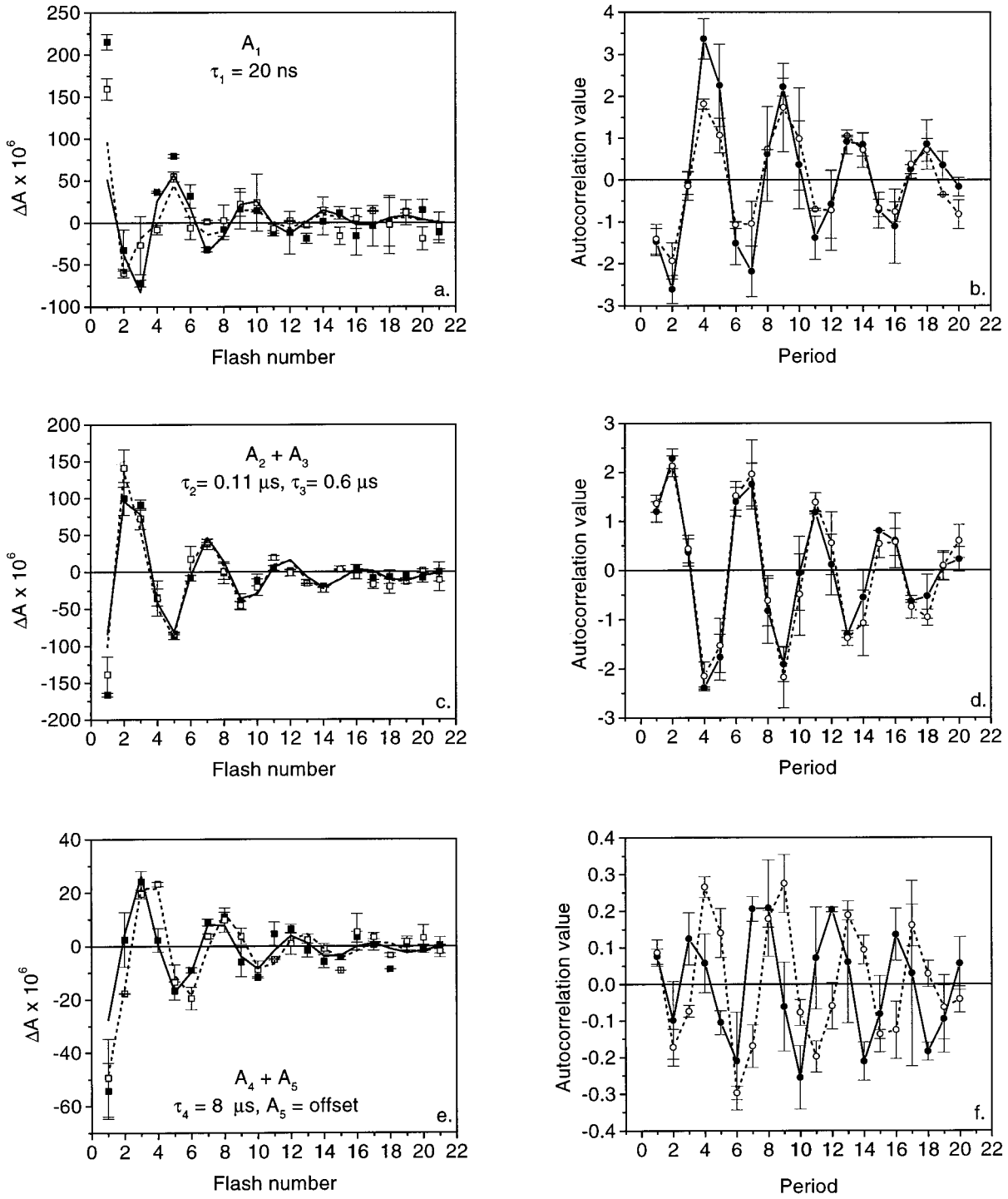

FIGURE 3: Kinetic components in the P680$^+$ reduction in H_2O and D_2O. Error bars indicate the spread of the results over duplicate experiments. Closed symbols, in H_2O; open symbols, in D_2O. (a, c, e) Components in the $\Delta A(t,n)$ curves (deviations from average, see Figure 2c,d). (b, d, f) Components in the $\Delta C(t,n)$ (autocorrelation curves). Lifetimes of components 1−4 in global analysis: τ_1, 20 ns; τ_2, 0.11 μs; τ_3, 0.6 μs; τ_4, 8 μs; A_5, offset. (a, b) A_1; (c, d) $A_{23} = A_2 + A_3$; (c, d) $A_{45} = A_4 + A_5$. Solid (in H_2O) and dashed lines (in D_2O) in (a), (c), and (e) indicate calculated amplitudes, obtained from an S-state decomposition of the observed amplitudes, using a miss factor of 0.18, both in H_2O and in D_2O. The lines in (b), (d), and (f) are merely drawn to guide the eye.

The effects of deuterium on P680$^+$ reduction kinetics in the time domain below 1 μs have been studied previously by two groups (*14*, *24*). Both groups report the absence of an isotope effect on P680$^+$ reduction on this time scale. However, Haumann et al. (*24*) found a large effect on the P680$^+$ reduction kinetics in particles that had been exposed to a high pH and had lost their oxygen-evolving capacity. The effect was particularly apparent in the microsecond time domain. Our observations are largely in agreement with these previously published data, in that there seems to be no significant isotope effect on the oscillatory phases with lifetimes below 1 μs.

Interpretation. Multiphasic P680$^+$ reduction kinetics are generally attributed to inhomogeneity in structure or energy levels within PS-II. It is highly likely that there will be inhomogeneity in a PS-II preparation, even within the population of particles that are fully active in oxygen evolution [e.g., (*12*, *13*)]. However, inhomogeneity cannot

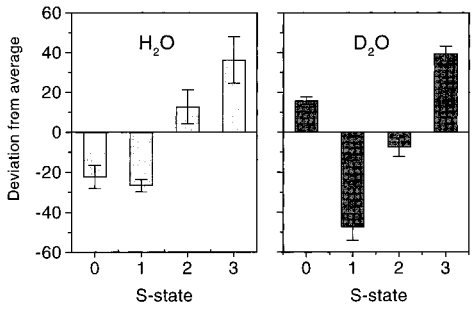

FIGURE 4: S-state decomposed amplitudes of the microsecond components (Figures 1b and 3e) in the $\Delta A(t,n)$ data sets. Left panel, in H_2O; right panel: in D_2O. Error bars indicate the spread of the decomposed amplitudes over 3 experiments in H_2O (data of Figures 1 and 3), and over 2 experiments in D_2O. Values on the horizontal axis indicate the S-state at the time of the excitation, i.e., before the transition.

be the explanation for the presence of nano- and microsecond phases in a single $P680^+$ reduction curve, for the following reasons. The range of lifetimes observed within single transitions varies from about 50 ns to 30 μs or more. According to nonadiabatic electron-transfer theory (*34*), this would mean a variation in distance between P680 and Y_Z of 1 nm, or a variation in the redox potential difference for the $P680^+/Y_Z^+$ couple of more than 500 meV. Such variations are far too large to be plausible and would significantly reduce the quantum yield of water splitting. Although heterogeneity in the protonation state of nearby residues might conceivably affect the redox potential of $P680^+$ and Y_Z^+ by 500 meV, it would still cause a severe loss of quantum yield in the water-splitting mechanism. Finally, the microsecond components cannot be explained by invoking a chain of electron donors to $P680^+$, because there is abundant evidence that Y_Z is the sole intermediate between P680 and the manganese cluster (*19*−*22*).

We propose that, in some of the S-state transitions, complete $P680^+$ reduction occurs in two distinct steps. The first step is rapid electron transfer from Y_Z to $P680^+$, and the equilibrium constant for the first step, $P680^+Y_Z \leftrightarrow P680Y_Z^+$ or $P680^+Y_Z \leftrightarrow P680Y_Z^\bullet$, is small [our data do not exclude the possibility that this first electron transfer is coupled to a proton-transfer event that is not rate-limiting, cf. (*22*)]. After the establishment of a quasi-equilibrium between the states, a measurable quantity of $P680^+$ still remains to be reduced. The second step, which occurs in 1−30 μs, causes further relaxation of the initially formed radical pair. Thus, in the S_0/S_1 and S_1/S_2 transitions Y_Z^+ or $Y_Z^\bullet$ reduction begins before $P680^+$ has been fully reduced (*23*). Therefore, it is likely that factors affecting the former reaction may also influence the latter.

A redox equilibrium between $P680^+$ and Y_Z^+ was proposed earlier by Brudvig and co-workers (*35*, *36*) in order to explain the oxidation kinetics of Y_D and cytochrome b_{559}, and by Shinkarev and Wraight (*37*, *38*), on the basis of the data presented by Witt and co-workers (*11*). However, their models do not specifically account for bi- or multiphasic reduction of $P680^+$.

Quantification of the $P680^+$ Concentration in the Microsecond Phases. Quantification of the isotope effect is only possible when certain assumptions are made, because the contribution of inactive centers to the isotope effect on the full $P680^+$ reduction is unknown.

An upper limit for the magnitude of the isotope effect is estimated on the basis of the following assumption. The microsecond components are smallest in the S_1/S_2 transition, both in H_2O and in D_2O. If we assume that $P680^+$ reduction during this transition has no microsecond component at all, then the absolute amplitudes of the other microsecond components may be calculated by subtracting A_{45} for S_1/S_2 from the other values of A_{45}. In that case, H_2O/D_2O exchange has a large effect on $P680^+$ reduction in the transition S_0/S_1 (A_{45} is 5−10 times higher in D_2O), and a smaller effect on the S_3/S_0 transition (A_{45} is 1.3 times higher in D_2O). However, it has no effect on the S_2/S_3 transition, which would imply that this particular proton/hydrogen transfer only occurs on the S_0/S_1 and S_3/S_0 transitions. This concurs with the findings of Rappaport et al. (*3*), who reported that electron transfer from the manganese cluster to Y_Z^+ in the transitions S_0/S_1 and S_3/S_0 was biphasic. In addition to an expected slow phase, there was a faster phase of about 25−50 μs, which the authors attributed to proton transfer or release.

It seems that the isotope effect which we observe on the microsecond phases of $P680^+$ reduction is related to intraprotein proton/hydrogen transfer rather than to proton release into the bulk. Haumann et al. (*2*) found that proton release can be as fast as 10 μs, but emphasize that this fast release rate is only observed under certain conditions. Under the conditions used in our experiments (pH 6.5), proton release into the bulk takes 100 μs (*39*). The isotope effect observed by us affects phases in the $P680^+$ reaction that are much faster than 100 μs. Therefore, the isotope effect observed by us must be associated with intraprotein proton/hydrogen transfer events.

Conclusions. On the basis of the observations presented in this paper, the following conclusions may be drawn. At least two processes play a role in the reduction of $P680^+$ by Y_Z. The fastest process occurs with time constants of tens to hundreds of nanoseconds and does not appear to be rate limited by proton/hydrogen transfer. In all or some of the S-state transitions (S_0/S_1, and possibly S_3/S_0), the slower processes involve proton/hydrogen motion, and occur in the microsecond time domain. These events occur before proton release to bulk, and are therefore intraprotein proton/hydrogen transfers.

ACKNOWLEDGMENT

We thank Dr. J. Lavergne (LBC-DEVM, CEA-Cadarache, 13108 Saint Paul lez Durance, France) for helpful discussions.

REFERENCES

1. Lavergne, J., and Junge, W. (1993) *Photosynth. Res. 38*, 279−296.
2. Haumann, M., and Junge, W. (1996) in *Oxygenic photosynthesis*: *the light reactions* (Ort, D. R., and Yocum, C. F., Eds.) pp 165−192, Kluwer Academic Publishers, Dordrecht, The Netherlands.
3. Rappaport, F., Blanchard-Desce, M., and Lavergne, J. (1994) *Biochim. Biophys. Acta 1184*, 178−192.
4. Bögershausen, O., and Junge, W. (1995) *Biochim. Biophys. Acta 1230*, 177−185.
5. Kretschmann, H., Schlodder, E., and Witt, H. T. (1996) *Biochim. Biophys. Acta 1274*, 1−8.

6. Britt, R. D. (1996) in *Oxygenic photosynthesis*: *the light reactions* (Ort, D. R., and Yocum, C. F., Eds.) pp 137−164, Kluwer Academic Publishers, Dordrecht, The Netherlands.
7. Diner, B. A., and Babcock, G. T. (1996) in *Oxygenic Photosynthesis*: *The light reactions* (Ort, D. R., and Yocum, C. F., Eds.) pp 213−247, Kluwer Academic Publishers, Dordrecht, The Netherlands.
8. Nugent, J. H. A. (1996) *Eur. J. Biochem. 237*, 519−531.
9. Debus, R. J. (1992) *Biochim. Biophys. Acta 1102*, 269−352.
10. Rutherford, A. W., Zimmerman, J.-L., and Boussac, A. (1992) in *The Photosystems*: *structure, function, and molecular biology* (Barber, J., Ed.) pp 179−229, Elsevier Science Publishers B. V., Amsterdam.
11. Brettel, K., Schlodder, E., and Witt, H. T. (1984) *Biochim. Biophys. Acta 766*, 403−415.
12. Meyer, B., Schlodder, E., Dekker, J. P., and Witt, H. T. (1989) *Biochim. Biophys. Acta 974*, 36−43.
13. Eckert, H.-J., and Renger, G. (1988) *FEBS Lett. 236*, 425−431.
14. Karge, M., Irrgang, K.-D., Sellin, S., Feinaugle, R., Liu, B., Eckert, H.-J., Eichler, H. J., and Renger, G. (1996) *FEBS Lett. 378*, 140−144.
15. Lukins, P. D., Post, A., Walker, P. J., and Larkum, A. W. D. (1996) *Photosynth. Res. 49*, 209−221.
16. Schlodder, E., Brettel, K., and Witt, H. T. (1985) *Biochim. Biophys. Acta 808*, 123−131.
17. Schlodder, E., and Meyer, B. (1987) *Biochim. Biophys. Acta 890*, 23−31.
18. Hoganson, C. W., Casey, P. A., and Hansson, O. (1991) *Biochim. Biophys. Acta 1057*, 399−406.
19. Barry, B. A., and Babcock, G. T. (1987) *Proc. Natl. Acad. Sci. U.S.A. 84*, 7099−7103.
20. Debus, J. R., Barry, B. A., Babcock, G. T., and McIntosh, L. (1988) *Proc. Natl. Acad. Sci. U.S.A. 85*, 427−430.
21. Debus, R. J., Barry, B. A., Sithole, I., Babcock, G. T., and McIntosh, L. (1988) *Biochemistry 27*, 9071−9074.
22. Gerken, S., Brettel, K., Schlodder, E., and Witt, H. T. (1988) *FEBS Lett. 237*, 69−75.
23. Razeghifard, M. R., Klughammer, C., and Pace, R. J. (1997) *Biochemistry 36*, 86−92.
24. Haumann, M., Bögershausen, O., Cherepanov, D., Ahlbrink, R., and Junge, W. (1997) *Photosynth. Res. 51*, 193−208.
25. Berthold, D. A., Babcock, G. T., and Yocum, C. F. (1981) *FEBS Lett. 134*, 231−234.
26. Ford, R. C., and Evans, M. C. W. (1983) *FEBS Lett. 160*, 159−164.
27. Rappaport, F., Porter, G., Barber, J., Klug, D., and Lavergne, J. (1995) in *Photosynthesis*: *from light to biosphere*. *Xth International Photosynthesis Congress* (Mathis, P., Ed.) pp 345−348, Kluwer Academic Publishers, Montpellier, France.
28. Schowen, R. L. (1977) in *Isotope effects on on enzyme catalyzed reactions* (Cleland, W. W., O'Leary, M. H., and Northrop, D. B., Eds.) University Park Press, Baltimore, MD.
29. Durrant, J. R., Giorgi, L. B., Barber, J., Klug, D. R., and Porter, G. (1990) *Biochim. Biophys. Acta 1017*.
30. Press, W. H., Flannery, B. P., Teukolsky, S. A., and Vetterling, W. T. (1989) *Numerical recipes. The art of scientific computing*, Cambridge University Press, Cambridge, U.K.
31. Marquardt, D. W. (1963) *J. Soc. Ind. Appl. Math. 2*, 431−441.
32. Lavergne, J. (1991) *Biochim. Biophys. Acta 1060*, 175−188.
33. Lavorel, J. (1978) *J. Theor. Biol. 57*, 171−185.
34. Marcus, R. A., and Sutin, N. (1985) *Biochim. Biophys. Acta 811*, 265−322.
35. Buser, C. A., Thompson, L. K., Diner, B. A., and Brudvig, G. W. (1990) *Biochemistry 29*, 8977−8985.
36. Buser, C. A., Diner, B. A., and Brudwig, G. W. (1992) *Biochemistry 31*, 11449−11459.
37. Shinkarev, V. P., and Wraight, C. A. (1993) *Photosynth. Res. 38*, 315−321.
38. Shinkarev, V. P., and Wraight, C. A. (1993) *Proc. Natl. Acad. Sci. U.S.A. 90*, 1834−1838.
39. Haumann, M., and Junge, W. (1994) *Biochemistry 33*, 864−872.

BI9713815